Clinical, Cosmetic and Investigational Dermatology

Dovepress
Taylor & Francis Group

Open Access Full Text Article

ORIGINAL RESEARCH

Integrative Analysis Reveals a Key Role for CDKN1A in Impaired Wound Healing in Diabetic Patients

Sis Aghayants[1,*], Shengzhi Zhou[1,*], Keyu Zhu[1,*], Zhixiang Tan[1], Bomin Cheng[2], Song Gong[3], Zhanyong Zhu[1]

[1]Department of Plastic Surgery, Renmin Hospital of Wuhan University, Wuhan, Hubei, 430060, People's Republic of China; [2]Chinese Medicine Health Management Center, Shenzhen Traditional Chinese Medicine Hospital, Shenzhen, People's Republic of China; [3]Division of Endocrinology, Tongji Hospital, Huazhong University of Science and Technology, Wuhan, Hubei 430030, People's Republic of China

*These authors contributed equally to this work

Correspondence: Bomin Cheng; Zhanyong Zhu, Email Szhyncbm@163.com; zyzhu@whu.edu.cn

Background: Diabetic foot ulcers (DFUs) are a common and severe complication of diabetes, often resulting in chronic non-healing wounds. This study aims to investigate the role of cyclin-dependent kinase inhibitor 1A (CDKN1A) in diabetic wound healing, focusing on its impact on cell proliferation and differentiation in DFUs.

Methods: We utilized single-cell RNA sequencing (scRNA-seq) to analyze gene expression profiles from DFUs tissues, comparing healing and non-healing groups. Differential gene expression analysis was performed to identify key regulators of wound healing. Mendelian randomization (MR) was employed to explore the causal relationship between CDKN1A expression and metabolic dysfunction in DFUs. Transcription factor analysis was also conducted to identify potential upstream regulators of CDKN1A.

Results: Our study confirmed that CDKN1A played a pivotal role in inhibiting cell proliferation and promoting premature differentiation in DFUs, which contributed to impaired wound healing. FOS was identified as a key transcription factor that upregulates CDKN1A in non-healing DFUs. MR analysis identified CDKN1A as being associated with metabolic changes, including the α-ketobutyrate/pyruvate ratio, leading to the impaired healing process in non-healing DFUs.

Conclusion: These findings shed light on the molecular mechanisms underlying DFU healing, suggesting that targeting FOS and CDKN1A could offer novel therapeutic strategies for enhancing wound healing in diabetic patients.

Keywords: diabetic foot ulcers, mendelian randomization, single-cell RNA sequencing, gene expression, CDKN1A, FOS

Introduction

Diabetic foot ulcers (DFUs) are a common complication of diabetes, often resulting in chronic non-healing wounds and significantly impacting the quality of life for diabetic patients.[1] Currently, 10.5% of adults aged 20 to 79 worldwide are living with diabetes, which accounts for 537 million people. Projections indicate that this number will rise to 643 million by 2030, with an expected increase to 783 million by 2045.[2] Between 15 and 25% of individuals with diabetes are expected to develop DFUs, which, along with amputations, represent major contributors to morbidity and mortality. Notably, 85% of diabetic amputees initially experience DFUs, which often progress to severe infections or gangrene.[3] The main factors impairing diabetic wound healing are increased blood glucose levels, oxygen deficiency, and excessive reactive oxygen species (ROS).[4] Current treatments for diabetic wound healing include blood sugar control, debridement, infection management with topical or systemic antibiotics, and the use of wound dressings. Additionally, therapies such as human growth factors, stem cells, and oxygen-based treatments, which have shown promise in improving wound healing, still need further experimental validation.[5] Hydrogels have emerged as a promising class of biomaterials for promoting diabetic wound healing due to their moisture-retentive properties, biocompatibility, and capacity for controlled drug delivery. Recently, a crosslinked multifunctional hydrogel based on naturally derived materials such as keratin, protocatechuic aldehyde, and iron ions was developed as a bioactive wound dressing. This hydrogel features a dual dynamic crosslinking network formed through thiol-aldehyde

Received: 16 April 2025
Accepted: 26 August 2025
Published: 4 September 2025

addition reactions and catechol–Fe^{3+} coordination, providing injectability, mechanical strength, self-healing ability, tissue adhesion, and antibacterial activity.[6] Another study demonstrated the effectiveness of a glucose-responsive gel loaded with glucose oxidase, catalase, Ce6, and NB, designed to eliminate drug-resistant pathogens and enhance the healing of refractory wounds. The enzymatic cascade enabled local oxygen generation, thereby enhancing photodynamic antibacterial activity in hypoxic environments while supporting tissue regeneration.[7] Despite significant research efforts, the detailed molecular mechanisms driving diabetic wound healing are still not fully understood, highlighting the need for deeper investigation into the genetic and metabolic pathways contributing to its development.

Recent advancements in single-cell RNA sequencing (scRNA-seq) have provided unprecedented insights into the cellular and molecular landscapes of complex biological processes, including diabetic wound healing.[8] scRNA-seq enables the identification of gene expression patterns at the resolution of individual cells, allowing for a deeper understanding of the variability in cell types in DFUs. The application of scRNA-seq in DFUs tissues to investigate molecular differences associated with impaired wound healing, such as the one by Theocharidis et al where scRNA-seq analysis was performed on healing and non-healing DFUs, along with forearm skin biopsies and PBMCs from both diabetic and healthy control groups.[9] These findings were further validated through immunostaining, spatial transcriptomics (ST), and in vitro experiments. For this study, we downloaded the scRNA-seq dataset from the Gene Expression Omnibus (GEO) database (GSE165816), which includes samples from both healed and unhealed DFUs.

It is worth noting that CDKN1A is a cyclin-dependent kinase inhibitor and regulates the cell cycle at the G1 phase, making it an essential factor in cell cycle control.[10] CDKN1A was first discovered to be a transcriptional target of p53.[11] CDKN1A regulation plays a significant role in various diseases, including diabetic wound healing. For instance, Su et al demonstrated that downregulating CDKN1A expression activates the Erk/Akt signaling pathway, promoting the proliferation and migration of fibroblasts exposed to high glucose (HG) conditions.[10] Abnormal CDKN1A expression in T2DM impairs insulin and glucagon secretion in clonal β- and α-cells, while promoter methylation reduces its transcriptional activity.[12] This disruption in cell cycle regulation at the G1 phase also compromises β-cell proliferation, exacerbating the metabolic dysfunction characteristic of T2DM.

Mendelian randomization (MR) is a genetic epidemiological approach that uses genetic variation as a natural experiment to make causal inferences about the relationship between risk factors and disease.[13] By capitalizing on the natural random allocation of alleles during meiosis. MR reduces confounding and eliminates reverse causation, common limitations in traditional observational studies.[14] Genetic variants associated with the exposure of interest serve as tools to infer whether changes in the exposure causally influence the outcome. This method has gained prominence in biomedical research for its robustness and ability to complement experimental findings, especially in exploring disease mechanisms and evaluating potential therapeutic targets.[15]

According to the above background, in this study, our primary aim was to investigate the critical role of cyclin-dependent kinase inhibitor 1A (CDKN1A) in DFUs using a combination of scRNA-seq and MR. We analyzed gene expression profiles from DFUs tissues to identify key regulators of wound healing and explored the causal relationship between CDKN1A expression and metabolic dysfunction in DFUs through MR analysis. Additionally, we conducted transcription factor analysis to uncover the regulatory network involving CDKN1A and its upstream regulators. The core conclusion of our study highlights CDKN1A as a pivotal regulator of wound healing in DFUs, shedding light on the molecular mechanisms underlying impaired healing (Figure 1). This study integrates single-cell transcriptomics with MR to investigate both the regulatory mechanisms and causal relationships underlying impaired wound healing in DFUs. By identifying CDKN1A as a central player and exploring its upstream transcriptional regulation by FOS, we present a multi-layered perspective that connects gene expression heterogeneity, transcriptional control, and metabolic pathways. This integrative approach advances the understanding of DFU pathophysiology and highlights potential therapeutic targets for improving wound healing outcomes in diabetic patients.

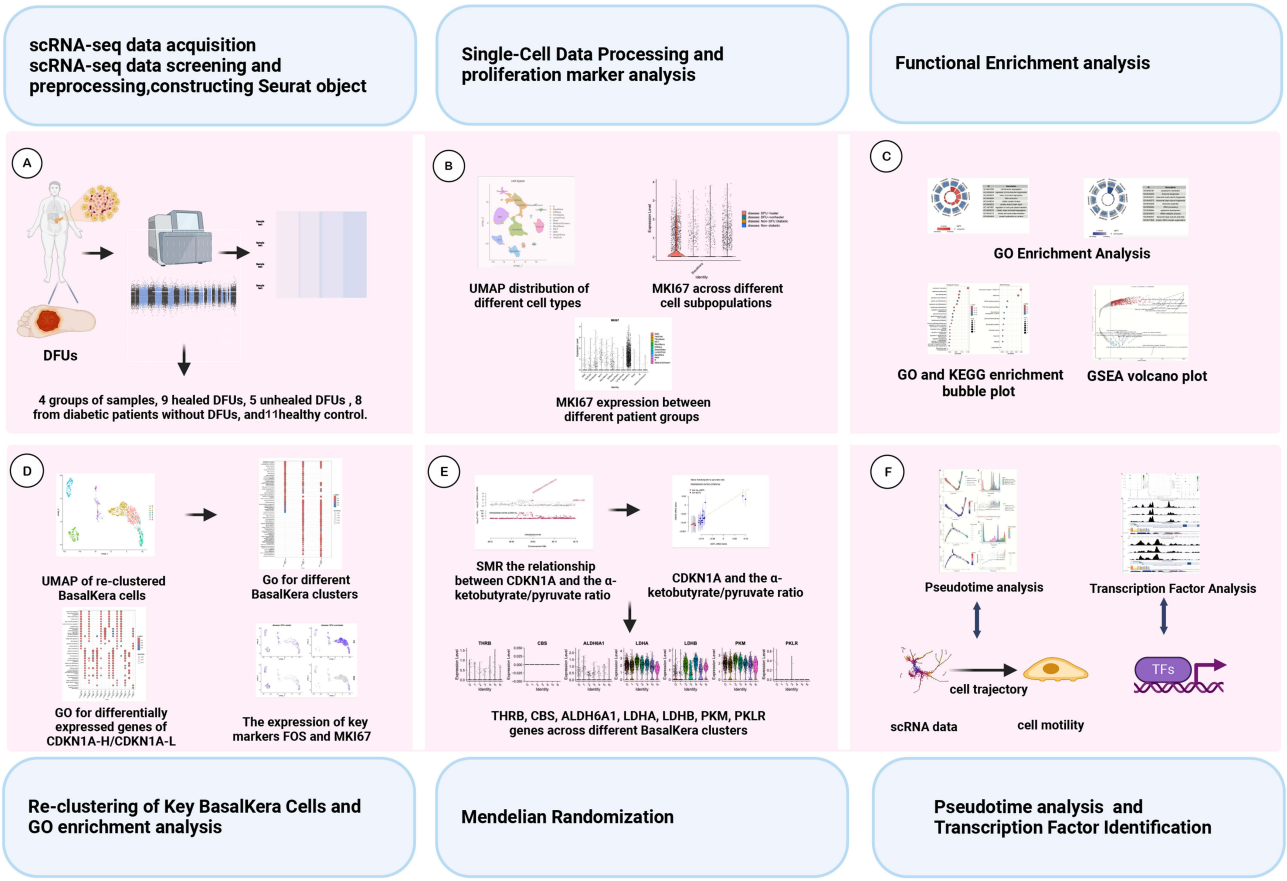

Figure 1 Workflow for identifying CDKN1A as a key regulator in DFU wound healing. (**A**) Data acquisition and preprocessing: Four groups of skin samples were collected, including healed DFUs (n=9), unhealed DFUs (n=5), diabetic patients without DFUs (n=8), and healthy controls (n=11). (**B**) Single-cell clustering and proliferation analysis: UMAP visualization shows cell-type distribution; MKI67 expression is analyzed across subpopulations and patient groups. (**C**) Functional enrichment analysis: GO and KEGG enrichment analyses were performed on differentially expressed genes, with visualization using bubble and volcano plots. (**D**) Re-clustering of BasalKera cells: UMAP plots and GO enrichment for CDKN1A-high/low groups; expression of key markers FOS and MKI67 shown. (**E**) Mendelian randomization analysis: SMR results link CDKN1A to α-ketobutyrate/pyruvate ratio; violin plots display expression of metabolism-related genes across BasalKera clusters. (**F**) Pseudotime and transcription factor analysis: Cell trajectory inferred from pseudotime analysis and identification of transcription factors potentially regulating wound healing processes.

Materials and Methods

Data Source

The scRNA-seq dataset for DFUs was downloaded from the GEO database (https://www.ncbi.nlm.nih.gov/gds), specifically the expression profile GSE165816. The selected samples include foot skin and control samples, with a total of 33 samples. These consist of 9 healed DFUs samples, 5 unhealed DFUs samples, 8 samples from diabetic patients without DFUs, and 11 healthy control samples from non-diabetic individuals. These samples were used for downstream analysis in this study.

For MR analysis, the outcome phenotype was DFUs, with relevant data obtained from the UK Biobank (UKB) database, a large-scale biomedical database. The exposure of interest was CDKN1A, with its expression quantitative trait loci (eQTL) data sourced from the IEU OpenGWAS database". (https://gwas.mrcieu.ac.uk/). Additionally, a dataset containing 1400 plasma metabolites was sourced from the GWAS Catalog (ID: GCST90199621-90,201,020).

Processing of Single-Cell Data for DFUs

The scRNA-seq data from GSE165816 underwent initial quality control (QC) processing, and no further QC screening was necessary. The data were processed using the Seurat package (v.5.0.1) in R software (v.4.3.2) (https://www.r-project.org/). To normalize the data, the NormalizeData() function was used, followed by the FindVariableFeatures() function (with nfeatures = 2500) to identify highly variable genes. Batch correction between samples was performed using the Harmony

package (v.1.2.0) in R to mitigate batch effects that could interfere with downstream analyses. Principal component analysis (PCA) was conducted for dimensionality reduction, selecting the top 35 principal components for further analysis. The FindNeighbors() and FindClusters() functions were used for cell clustering at a resolution of 0.5. Cell annotation utilized the cell type annotation information provided by the original authors of the dataset.[9]

Expression Analysis of Key Markers

The expression of MKI67, a marker of cell proliferation, across various subpopulations was visualized using the Seurat package in R. To investigate the expression of tissue mobility-related genes (FOS, FOSB, JUN, JUNB, EREG, EGFR, MAP2K1, MAP2K2), the myosin-related gene MYH9, and the cell adhesion-related gene CDH1,[16] we performed differential expression analysis between the healed and unhealed DFUs groups. This analysis was conducted using the FindMarkers() function in Seurat, combined with the limma package (v.3.58.1) in R. The results were visualized using ggplot2 (v.3.5.1).

Functional Enrichment Analysis

Next, we performed differential expression analysis using the FindMarkers() function from the Seurat package on key cell subpopulations, specifically basal keratinocytes (BasalKera), in both the healed and unhealed DFUs groups. The criteria for selecting differentially expressed genes (DEGs) were p_val_adj < 0.05. Upregulation and downregulation of genes were determined based on the value of avg_log2FC: DEGs with avg_log2FC > 0 were considered upregulated, while those with avg_log2FC < 0 were considered downregulated.

Subsequently, we conducted Gene Ontology (GO) enrichment analysis for both upregulated and downregulated DEGs using the clusterProfiler package in R. The analysis primarily focused on biological processes (BP), with a filtering criterion of qvalueCutoff = 0.05, while other parameters were kept at their default settings. Key pathways were visualized as circular plots using the GOplot package (v.1.0.2). Additionally, Gene Set Enrichment Analysis (GSEA) based on GO enrichment was performed using clusterProfiler, and the results were visualized as a volcano plot using the GseaVis package (v.0.1.0).

Then, BasalKera cells were divided into two groups based on the median expression value of the tissue mobility-related gene FOS: high expression (FOS-H) and low expression (FOS-L). Cells with FOS expression greater than the median were classified as FOS-H. We then conducted differential expression analysis using the FindMarkers() function for the FOS-H/FOS-L groups in the healed DFU group and repeated the same analysis for the unhealed DFU group, applying the same selection criterion (p_val_adj < 0.05). The intersection of the results from both differential analyses was used to identify overlapping DEGs. The GO and KEGG enrichment analyses were performed on these overlapping DEGs using the clusterProfiler package, with the same pathway selection criteria. The results were visualized as a bubble plot using the clusterProfiler package.

Re-Clustering of BasalKera

Re-clustering of BasalKera was performed using the Seurat package, removing outlier clusters and clusters with very few cells. To eliminate batch effects, the Harmony package (v.1.2.0) was applied, and dimensionality reduction clustering was performed using PCA, selecting the top 10 principal components (PCs) for subsequent analysis. The resolution was set to 0.3, with other parameters at their default values. For single-cell differential analysis on the clustered data, the FindAllMarkers() function from the Seurat package was used, applying a selection criterion of p_val_adj < 0.05. Sample proportions within the clusters were examined to understand the distribution of sample types. Additionally, the expression levels of FOS and MKI67 were assessed to determine whether their expression trends were consistent with the sample proportion trends. Enrichment analysis on the DEGs in the clusters was performed using the clusterProfiler package, focusing on the Gene Ontology biological processes (GO.BP) pathways associated with clusters that had a high proportion of unhealed DFUs samples. Key pathways were selected, and the core genes within two of these pathways were visualized using the graph package (v.2.0.1.1) to identify critical genes.

Differential Enrichment Analysis of CDKN1A High and Low Expression Groups in BasalKera

BasalKera were classified into two groups based on the expression levels of the key gene CDKN1A: the CDKN1A high expression group (CDKN1A-H), where expression values were greater than 0, and the CDKN1A low expression group (CDKN1A-L). Using the FindMarkers() function from the Seurat package, we performed differential expression analysis between the CDKN1A-H and CDKN1A-L groups in both the healed and unhealed DFUs groups, applying a DEGs selection criterion of $p < 0.05$. We then conducted GO enrichment analysis on the upregulated and downregulated DEGs in both the healed and unhealed groups using the clusterProfiler package, maintaining the same pathway selection criteria as in previous analyses.

Mendelian Randomization (MR)

This study employed MR to perform mediation analysis using plasma metabolites as both exposure and outcome in two separate MR analyses. We utilized the TwoSampleMR package (v.0.6.7) in R to select instrumental variables, applying the following selection criteria: $p < 1e\text{-}5$, $r^2 = 0.001$, and clump_kb = 10,000 kb. The mr() function in TwoSampleMR was used to perform MR analysis between plasma metabolites and DFUs to identify causal metabolites.

In addition, we used SMR software (v.1.3.1) to conduct SMR analysis between CDKN1A and plasma metabolites, as well as between CDKN1A and DFUs. When performing MR analysis with the TwoSampleMR package, we applied five algorithms: Inverse Variance Weighted (IVW), MR-Egger, Weighted Median, Simple Mode, and Weighted Mode. The primary results of the MR analysis were based on the IVW method. Heterogeneity analysis was conducted using Cochran's Q test. In cases of heterogeneity, a random effects IVW model was applied; otherwise, a fixed effects IVW model was used.

Sensitivity analysis was conducted, including tests for heterogeneity and horizontal pleiotropy. The presence of pleiotropy was evaluated using the MR-Egger intercept, with $P > 0.05$ indicating no horizontal pleiotropy. The MR-PRESSO method was further applied to assess pleiotropy, and the leave-one-out method was used to evaluate the robustness of the results by sequentially removing one genetic variant at a time.

Pseudotime Analysis

Two key cell types were selected for pseudotime analysis: BasalKera, representing undifferentiated cells, and differentiating keratinocytes (DiffKera), representing differentiated cells. These cell populations were merged and analyzed for pseudotime trajectory reconstruction using the monocle2 package (v.2.30.0). Additionally, pseudotime analysis was performed on the reclustered BasalKera data to further explore differentiation trajectories. The expression patterns of CDKN1A were examined in both pseudotime analyses.

Transcription Factor Analysis

The pyscenic package (v.0.12.1) was used to analyze transcription factors in BasalKera cells, identifying differences between healed and unhealed DFUs groups. Transcription factor expression was also analyzed across different clusters in the reclustered data. To assess the overall functional characteristics of reclustered BasalKera cells, PCA was performed using the ReactomeGSA package (v.1.16.1). The Cistrome database was examined to determine if transcription factors FOS and JUNB exhibited peak enrichment at the CDKN1A locus.

Results

Single-Cell Analysis of DFUs Reveals the Cellular Landscape at Different Stages of the Disease

After preprocessing the scRNA-seq data from DFUs, a total of 94,325 cells and 26,923 genes were obtained. Unsupervised clustering identified 27 distinct clusters (Figure 2A). The expression distributions of marker genes for each cell type were visualized using a bubble plot (Figure 2B). After annotating the cell types, we identified 12 distinct cell types, including smooth muscle cells (SMC), vascular endothelial cells (VasEndo), fibroblasts, NK/T cells,

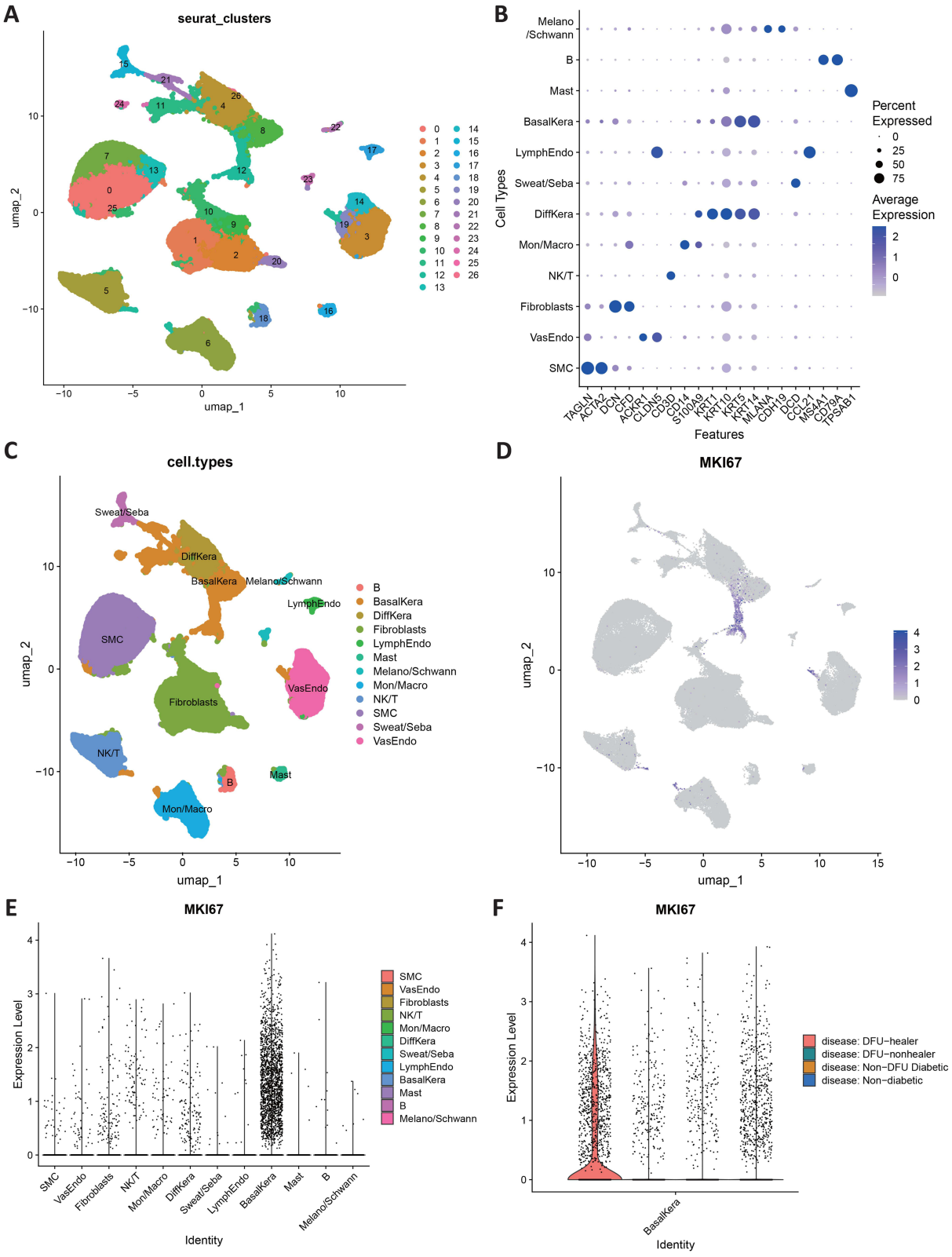

Figure 2 Cellular landscape of DFUs at different disease stages. (**A**) Uniform Manifold Approximation and Projection (UMAP) distribution of single-cell RNA-seq (scRNA-seq) data generated through unsupervised clustering. (**B**) Bubble plot showing the distribution of cell type marker genes, where bubble size indicates the proportion of cells expressing each gene and color intensity represents the average expression level. (**C**) UMAP distribution of different cell types. (**D**) Feature plot showing the expression of MKI67, a key proliferation marker. (**E**) Violin plot illustrating the expression of MKI67 across different cell subpopulations. (**F**) Violin plot comparing MKI67 expression between different patient groups.
Abbreviations: UMAP, Uniform Manifold Approximation and Projection; scRNA-seq, single-cell RNA sequencing.

monocytes/macrophages, DiffKera, sweat/sebaceous glands (Sweat/Seba), lymphatic endothelial cells (LymphEndo), BasalKera, mast cells, B cells, and melanocytes/Schwann cells (Melano/Schwann). The distribution of these cell types was visualized using Uniform Manifold Approximation and Projection (UMAP) (Figure 2C). Simultaneously, the key marker for cell proliferation, MKI67, was used to examine proliferation (Figure 2D and E). MKI67 was found to be highly expressed in BasalKera cells, particularly in the healing DFUs group, with no significant differences observed in the other cell types or disease stages (Figure 2F). Histological staining from the original dataset confirmed that both the non-healing DFUs group and the healing DFUs group had ulcerated wounds. Based on these observations, we focused the subsequent analysis on the comparison between the healing and non-healing DFUs groups.

Expression of Genes Related to Tissue Fluidity and Functional Enrichment

Recent findings highlight that skin tissue repair during wound healing is dynamically regulated by tissue fluidity, with early-stage fluidization driven by cell proliferation and changes in cell adhesion, involving key factors like EGFR-AP-1, JUN, FOS, MYH9, and CDH1.[16] Then, we analyzed the differential expression of these genes in the DFU healing and non-healing groups (Figure 3A). The results revealed that FOS and JUNB were significantly downregulated in the healing DFU group but upregulated in the non-healing DFUs group, indicating that high expression of these genes may inhibit tissue fluidity. Additionally, MYH9 was highly expressed in the healing DFU group, further suggesting that tissue fluidity was enhanced in the healing group but suppressed in the non-healing group.

Subsequently, we performed an enrichment analysis of upregulated and downregulated genes in the BasalKera cells from both the healing and non-healing DFU groups. The upregulated genes were mainly enriched in pathways related to cell division, bacterial and viral infections, and the TNF signaling pathway, while the downregulated genes were primarily enriched in pathways related to ribosomes, humoral immune responses, p53 signaling, and epidermal differentiation and development (Figure 3B and C). Thus, in BasalKera cells, differentiation functions were active in the non-healing DFUs group, but cell replication was suppressed.

To validate these findings, we conducted a GSEA analysis, which confirmed that cell differentiation, humoral immunity, the p53-mediated p21 pathway, and ribosome-related pathways were highly enriched in the non-healing DFUs group (Figure 3D). The wound healing process in non-healing DFU patients exhibited abnormalities, with cell proliferation and tissue fluidity necessary for density recovery being inhibited, while cell differentiation occurred prematurely, before cell density recovery.

Finally, BasalKera cells were categorized in the healing and non-healing DFU groups into high-FOS and low-FOS subgroups based on the median expression of FOS. Differential analysis was performed between the high-FOS and low-FOS groups in both the healing and non-healing groups. The intersection of the upregulated genes in both groups was functionally enriched, revealing key pathways associated with cell differentiation, p53 signaling, and other processes, suggesting that high FOS expression in DFUs patients impacts cell differentiation and p53 signaling (Figure 3E).

Re-Clustering of Key BasalKera Cells

To further explore differences in BasalKera cells between the DFUs healing and non-healing groups, we performed a re-clustering analysis on BasalKera cells from both groups. After removing outlier clusters and clusters with too few cells, we identified a total of seven clusters (Figure 4A). The bar plot representing cell proportions shows that in clusters 0, 1, 3, and 5, there is a higher proportion of cells from the non-healing DFUs samples. In clusters 2 and 4, a higher proportion of cells come from the healing DFUs samples, while cluster 6 contains nearly equal proportions of healing and non-healing DFUs samples (Figure 4B).

Enrichment analysis results indicated that upregulated genes in clusters 2, 3, and 4 were mainly enriched in chromosome-related terms, while upregulated genes in clusters 0, 1, and 5 were primarily enriched in pathways related to ribosomes, cell differentiation, and the p53 signaling pathway (Figure 4C). In cluster 3, upregulated genes were mainly associated with chromosome-related and cell differentiation-related terms. Cluster 6 was enriched in terms related to gland morphogenesis, muscle contraction, regulation of neural differentiation, glomerulus development, and nephron development. Based on the cell proportions, we hypothesize that the functional enrichment results for clusters 3 and 6 are influenced by the similar proportions of healing and non-healing DFUs samples in these clusters. We also examined the expression of FOS and MKI67. Clusters 0,

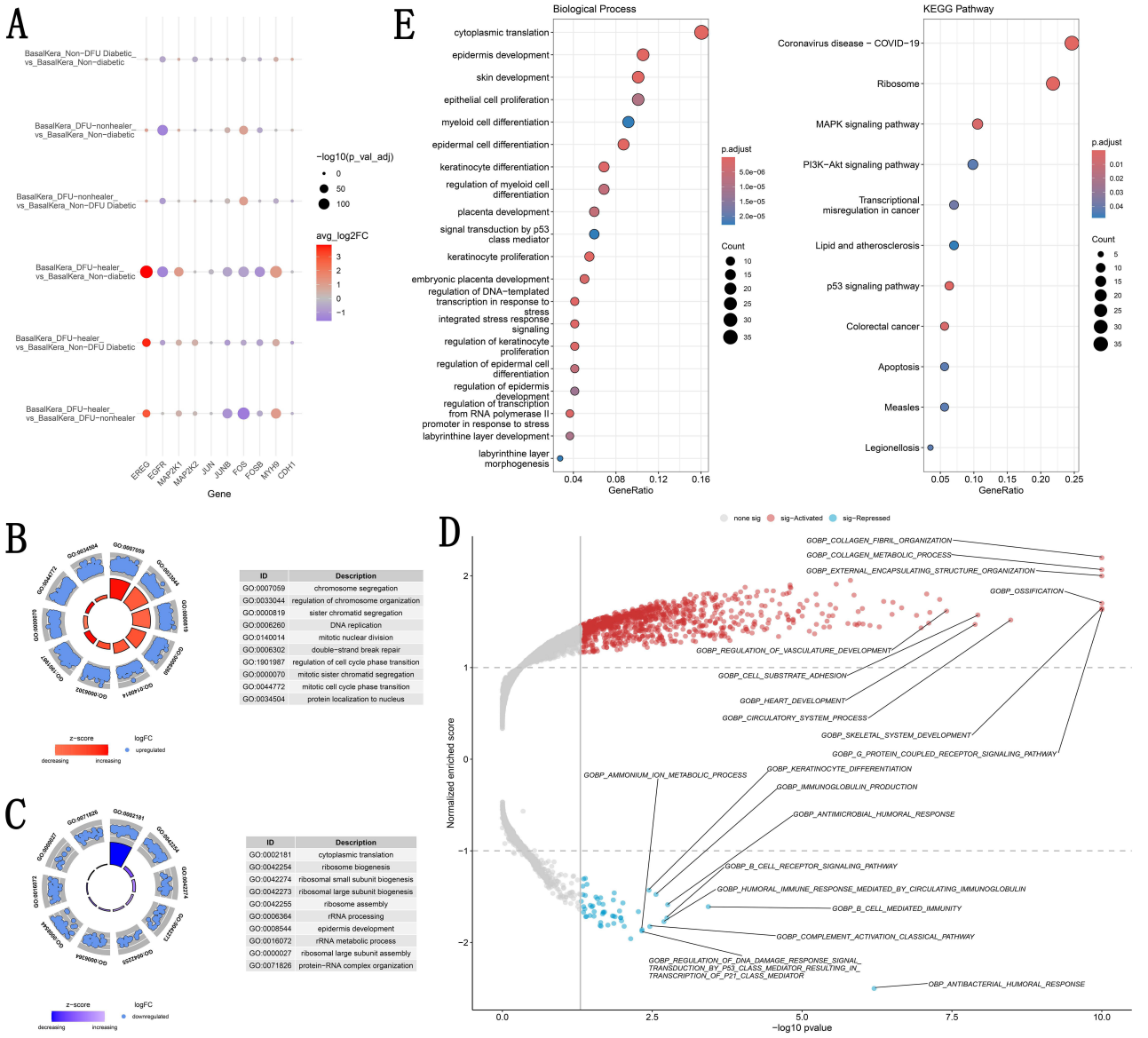

Figure 3 Differential expression and functional enrichment of tissue fluidity-related genes. (**A**) Bubble plot showing the differential expression of tissue fluidity-related genes across comparisons. Circle size represents the adjusted p-value (−log10), and color indicates average log2 fold change (log2FC). (**B**) Circular plot of Gene Ontology (GO) enrichment for upregulated differentially expressed genes (DEGs) between the DFUs healing and non-healing groups. The outer ring shows log2FC, and the inner colored bars represent Z-scores. Red indicates upregulation. (**C**) Circular plot of GO enrichment for downregulated DEGs between the DFUs healing and non-healing groups. Similar to (B), the outer ring displays log2FC, and the inner blue bars show negative Z-scores indicating downregulation. (**D**) Gene Set Enrichment Analysis (GSEA) volcano plot for the non-healing DFUs group, based on GO enrichment results. The x-axis shows −log10(p-value), and the y-axis shows normalized enrichment scores (NES). Red points represent significantly upregulated gene sets; blue points indicate significantly downregulated gene sets. Representative gene ontology terms are labeled. (**E**) GO Biological Process and KEGG Pathway enrichment results for upregulated DEGs shared between the high and low FOS expression groups. Dot size reflects gene count; color indicates adjusted p-value (p.adjust).

Abbreviations: GO, Gene Ontology; DEGs, differentially expressed genes; GSEA, Gene Set Enrichment Analysis.

1, 3, 5, and 6 exhibited high expression of FOS, with the highest expression observed in clusters 0 and 1, especially in the non-healing DFUs group (Figure 4D). MKI67 expression was high in clusters 2 and 4, with higher expression observed in the healing DFUs group (Figure 4E). These expression patterns of FOS and MKI67 are consistent with the results of previous analyses. Therefore, through enrichment analysis of cells with high and low CDKN1A expression, we found that cells with high CDKN1A expression are significantly linked to energy metabolism (Figure 4F).

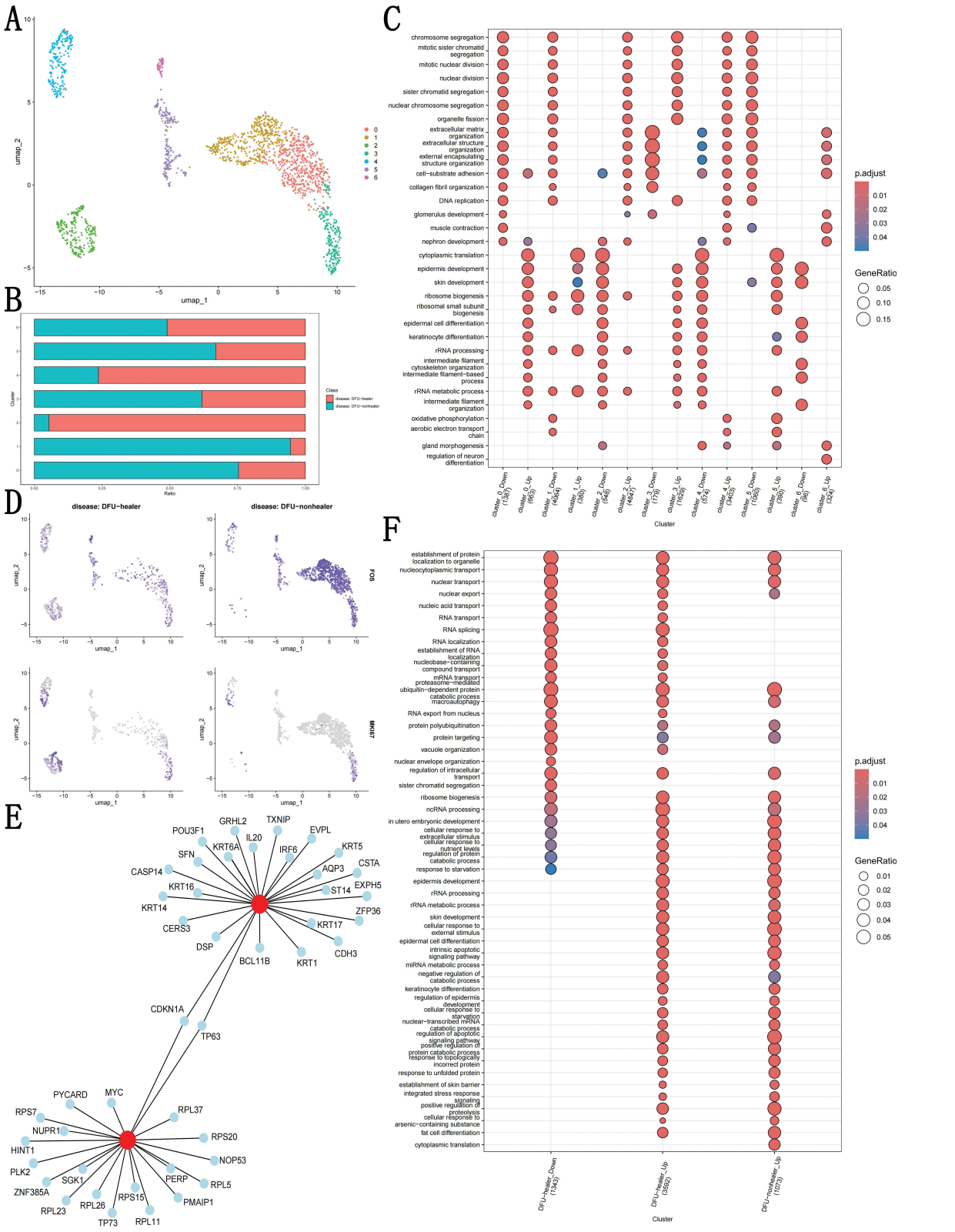

Figure 4 Re-clustering of BasalKera cells and identification and functional enrichment of CDKN1A. (**A**) UMAP distribution of re-clustered BasalKera cells. (**B**) Bar plot showing the proportion of cells in each BasalKera cluster. (**C**) Bubble plot of GO enrichment analysis for different BasalKera clusters. (**D**) Feature plots showing the expression of key markers FOS and MKI67 between different groups. (**E**) Network diagram of core genes associated with two enriched pathways: keratinocyte differentiation and signal transduction by p53 class mediator. Red nodes represent pathway hubs, and blue nodes represent interacting genes. (**F**) GO enrichment bubble plot for differentially expressed genes between high and low CDKN1A expression groups.

https://doi.org/10.2147/CCID.S534876

Mendelian Randomization (MR) Analysis

Given the known association between DFUs and metabolic processes, MR analysis was first conducted to explore the causal relationship between 1400 metabolites and DFUs. The MR analysis aimed to determine if changes in metabolite levels directly influence the risk of developing or worsening DFUs. After performing sensitivity tests and excluding exposures with horizontal pleiotropy, the MR results revealed that 43 metabolites were causally related to DFUs (Figure 5A). These results were validated with sensitivity tests, which confirmed no heterogeneity or horizontal pleiotropy in the exposures, and no significant bias was detected in the SNPs (Table S1, Table S2).

Next, Summary-data-based Mendelian Randomization (SMR) analysis was performed to assess the relationship between CDKN1A and DFUs, as well as between CDKN1A and the 43 metabolites identified in the MR analysis. The SMR analysis showed no significant causal relationship between CDKN1A and DFUs (pSMR > 0.05). However, when examining the eQTL of CDKN1A and the 43 metabolites, we found a significant causal relationship between CDKN1A and the ratio of α-ketobutyrate to pyruvate. Specifically, CDKN1A was identified as a risk factor for the α-ketobutyrate/pyruvate ratio (with a positive slope in the SMR effect plot) (Figure 5B and C). Moreover, both α-ketobutyrate and pyruvate ratios were shown to be risk factors for DFUs (OR > 1). Given that CDKN1A is more highly expressed in the non-healing DFUs group, it is likely that the effect of CDKN1A on DFUs is mediated by the α-ketobutyrate/pyruvate ratio, establishing a mediated causal relationship between CDKN1A, the α-ketobutyrate/pyruvate ratio, and DFUs.

We further investigated the expression of genes associated with α-ketobutyrate (THRB, CBS, ALDH6A1) and found no significant differences in their synthesis or breakdown across BasalKera clusters. In contrast, genes related to pyruvate, such as LDHA and LDHB, showed relatively higher expression in clusters 2 and 4, which were associated with the healing DFUs group (Figure 5D). On the other hand, PKM and PKLR did not show notable expression differences, but their expression was higher in the healing group. Consequently, pyruvate-related genes had lower expression in the non-healing DFUs group, while the α-ketobutyrate/pyruvate ratio was higher, which was consistent with the MR findings. Since pyruvate is closely linked to energy metabolism and can be converted into acetyl-CoA in the mitochondrial matrix to enter the TCA cycle,[17,18] these findings suggest a crucial role for CDKN1A in regulating DFU wound healing through energy metabolism. In summary, CDKN1A influences DFU wound healing through its role in energy metabolism, specifically via the α-ketobutyrate/pyruvate ratio.

Pseudotime Analysis

The pseudotime analysis was conducted to examine the differentiation trajectories of BasalKera and DiffKera cells from the DFUs healing and DFUs non-healing groups. The results revealed distinct differentiation states in the healing group: BasalKera and DiffKera cells were predominantly located in the starting region of differentiation on the left and the terminal differentiation region on the right (Figure 6A and B). In contrast, in the non-healing group, both BasalKera and DiffKera cells were concentrated in the middle region of differentiation. This suggests that the intracellular functions of BasalKera and DiffKera cells in the non-healing group are impaired.

The relatively higher differentiation status of BasalKera cells in the non-healing group aligns with previous enrichment analysis findings, indicating abnormal differentiation. Moreover, there were fewer fully differentiated DiffKera cells in the non-healing group, suggesting incomplete functionality, which may be linked to impaired energy metabolism. CDKN1A expression was higher in fully differentiated cells, and its overall expression was relatively higher in the non-healing group, correlating with the observed differentiation states (Figure 6C).

To further investigate, we performed pseudotime analysis on the reclustered BasalKera cells. The differentiation trajectory curve revealed that clusters 2 and 4 were situated in the starting region of differentiation, while clusters 0 and 1 were in the terminal region (Figure 6D and E). Combined with differences in cell proportions across clusters, the degree of BasalKera cell differentiation was higher in the non-healing group compared to the healing group. Furthermore, CDKN1A expression was observed to increase gradually along the differentiation trajectory, with significantly higher levels in the non-healing group, consistent with previous findings (Figure 6F).

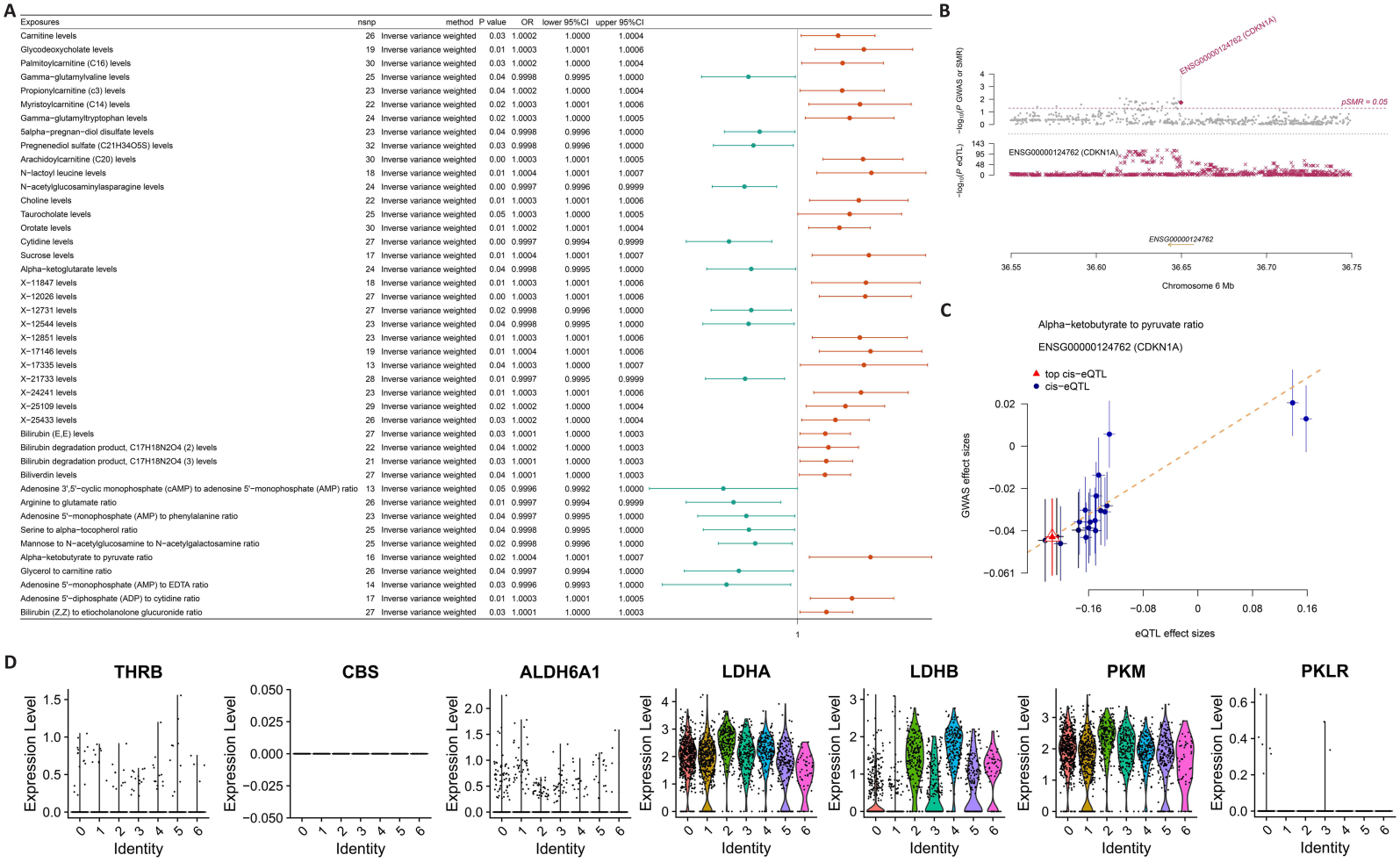

Figure 5 Mediation MR results and expression of genes involved in the synthesis and breakdown of α-ketobutyrate and pyruvate. (**A**) Forest plot of Mendelian Randomization (MR) analysis for 1400 metabolites associated with diabetic foot ulcers (DFUs). (**B**) Summary-data-based Mendelian Randomization (SMR) Manhattan plot showing the relationship between CDKN1A and the α-ketobutyrate/pyruvate ratio. The upper gray points indicate SMR p-values, while the lower pink points represent corresponding eQTL p-values. (**C**) SMR effect plot demonstrating the causal relationship between CDKN1A and the α-ketobutyrate/pyruvate ratio. (**D**) Violin plots showing the expression levels of genes involved in α-ketobutyrate synthesis (THRB, CBS, ALDH6A1) and pyruvate metabolism (LDHA, LDHB, PKM, PKLR) across different BasalKera clusters.

https://doi.org/10.2147/CCID.S534876

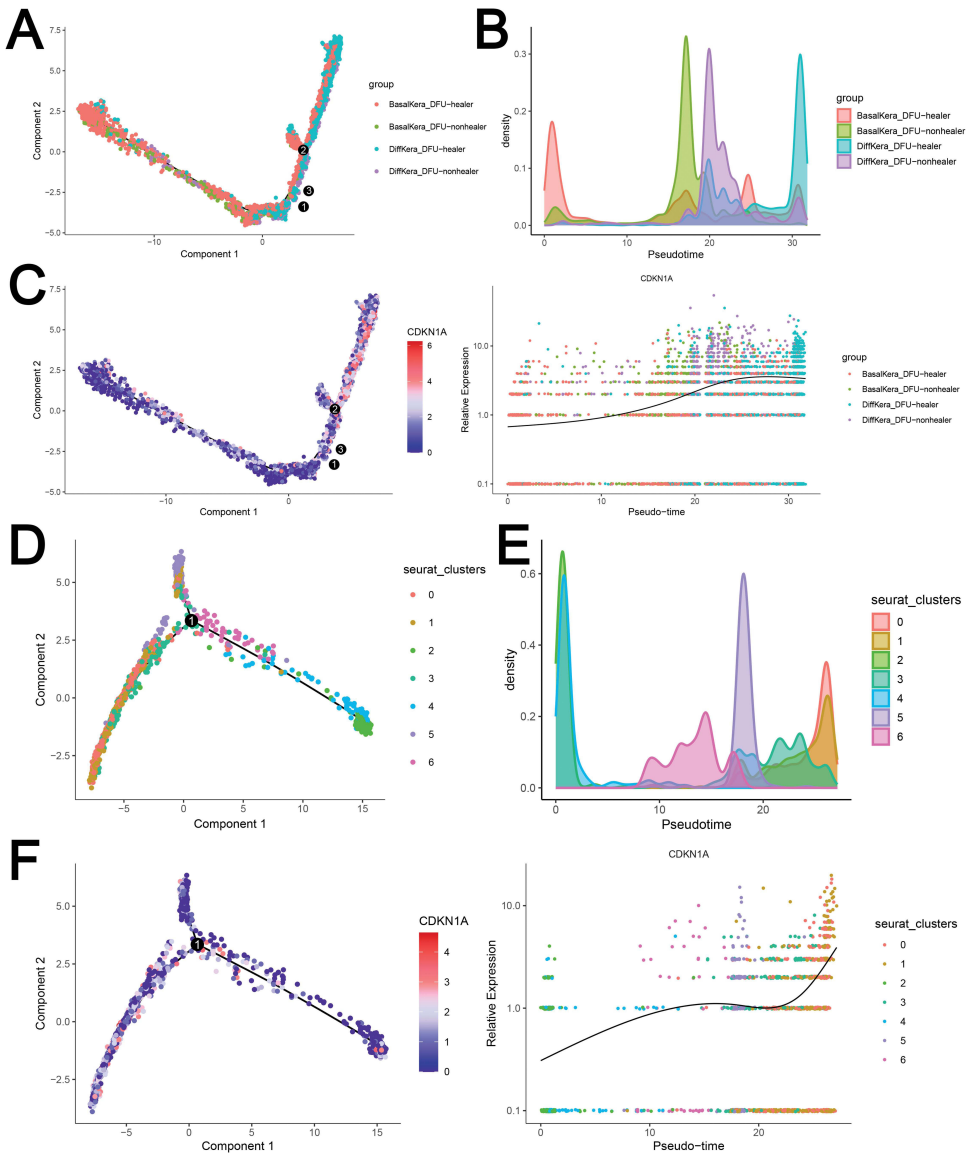

Figure 6 Pseudotime analysis of key cells. (**A**) Pseudotime trajectory of BasalKera and DiffKera cells from the DFUs healing and non-healing groups. (**B**) Density distribution of BasalKera and DiffKera cells along pseudotime for different groups. (**C**) Expression trajectory plot (left) and pseudotime expression curve (right) of CDKN1A in BasalKera and DiffKera cells across different groups. (**D**) Pseudotime trajectory of reclustered BasalKera cells. (**E**) Density distribution of reclustered BasalKera cells along pseudotime. (**F**) Expression trajectory plot (left) and pseudotime expression curve (right) of CDKN1A in reclustered BasalKera cells. The black numeric circles (eg, 1, 2, 3) represent the various cell states identified by Monocle, reflecting different stages in the differentiation process of keratinocytes.

Transcription Factor Analysis

The analysis revealed that FOS and JUNB regulate a larger number of genes in the non-healing group compared to the healing group (Figure 7A). PCA showed that clusters 1, 5, and 6 were found to have similar functional profiles, as were clusters 2 and 4 (Figure 7B). Based on these observations, we merged clusters with similar functions into four groups for subsequent analysis: 1-5-6, 2–4, 0, and 3. Transcription factors in the four merged BasalKera cluster groups showed that in the 1-5-6 group, transcription factors TP63, FOS, JUN, and JUNB, were identified as key regulators, with similar results observed in cluster 0 (Figure 7C).

Combining these findings with previous analyses of differentially expressed genes related to tissue fluidity, we observed that the transcription factors FOS and JUNB have more regulatory influence in the non-healing group. Subsequently, we checked the peak profiles for transcription factors FOS and JUNB in the cistrome database (using epithelial tissue as the reference). The key gene CDKN1A shows strong peak values for both FOS and JUNB, with

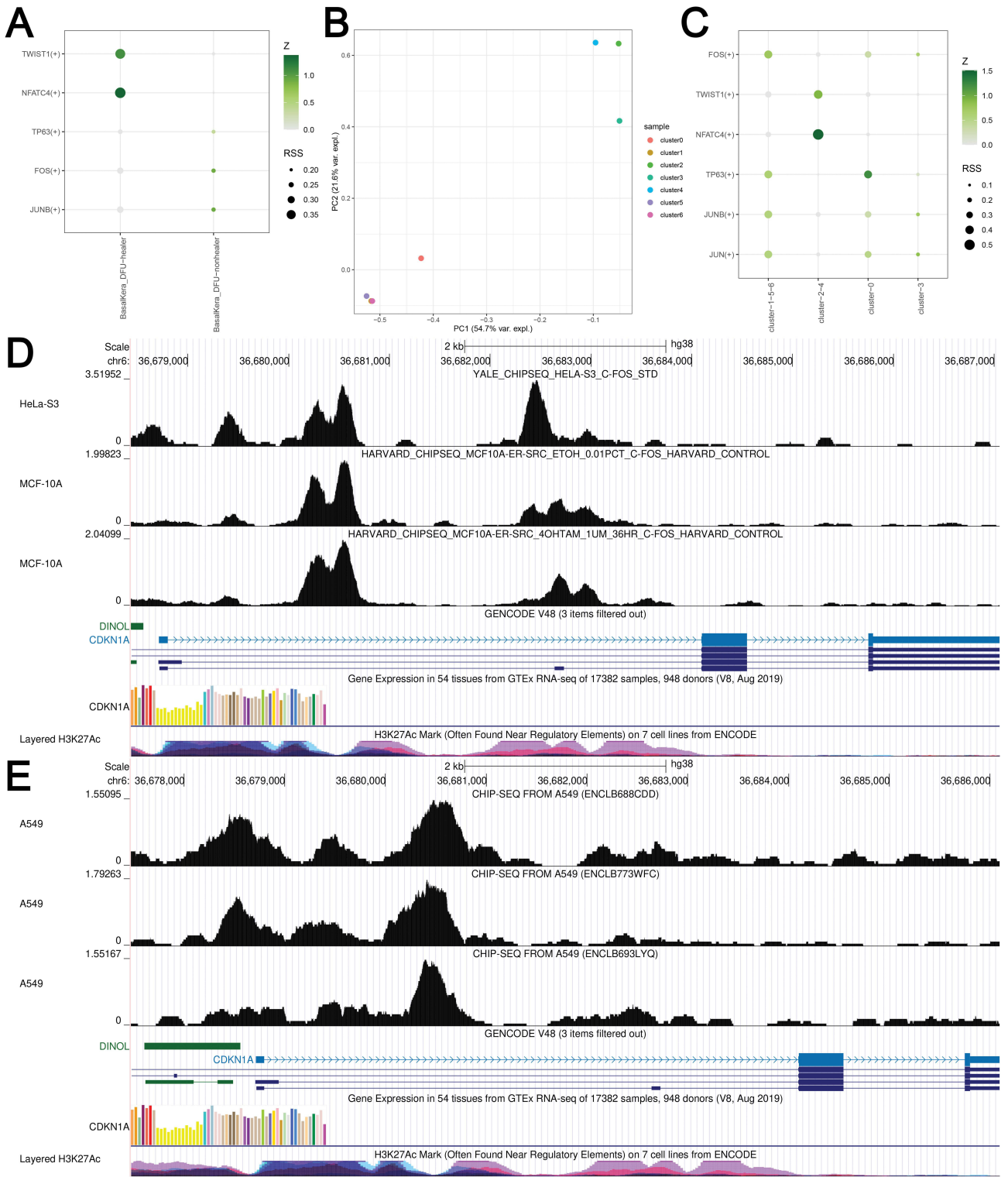

Figure 7 Transcription Factor Analysis. (**A**) Bubble plot showing differentially expressed transcription factors in BasalKera cells between the DFUs healing and non-healing groups. (**B**) PCA plot illustrating functional differences among reclustered BasalKera cell groups, highlighting similarities and differences across clusters. (**C**) Bubble plot displaying differentially expressed transcription factors across BasalKera clusters. (**D**) ChIP-seq tracks for CDKN1A demonstrating open peak regions under regulation by FOS in epithelial tissues. (**E**) ChIP-seq tracks for CDKN1A demonstrating open peak regions under regulation by JUNB in epithelial tissues, validating their transcriptional regulatory influence on CDKN1A.

https://doi.org/10.2147/CCID.S534876

a particularly high open peak in FOS, indicating that both FOS and JUNB have transcriptional regulatory effects on CDKN1A, with FOS showing a relatively stronger effect (Figure 7D and E).

Discussion

DFUs are a prevalent and serious complication of diabetes, with chronic non-healing wounds significantly contributing to patient morbidity and mortality.[19,20] Despite progress in wound care and therapeutic interventions, impaired molecular mechanisms in DFUs, such as dysregulated inflammatory responses, impaired angiogenesis, and fibroblast and keratinocyte dysfunction, remain poorly understood.[21,22] MR can help uncover these mechanisms and pathways by identifying causal relationships that directly impact disease progression.[23] In this study, we adopted an integrative approach that combined scRNA-seq, MR, and enrichment analysis. Our results highlight the pivotal roles of tissue fluidity, CDKN1A, and interconnected metabolic and transcriptional regulatory networks in the diabetic wound healing process.

In our study, samples were collected from healed DFU cases, unhealed DFU cases, diabetic patients without DFUs, and healthy controls. To assess cell proliferation, we focused on MKI67, a well-established biomarker for cell proliferation. MKI67, encoding Ki-67, is crucial for cellular proliferation and plays a significant role in tissue regeneration, particularly in wound healing.[24] Studies have consistently shown elevated Ki-67 expression at the wound edge, indicating active cell proliferation.[25] Specifically, in our study, BasalKera cells exhibited high MKI67 expression, with the healing DFUs group showing the highest levels. Conversely, MKI67 expression in the other groups remained within normal ranges without significant differences.

Secondly, recent studies have emphasized the significance of tissue fluidity in facilitating cell and tissue adaptability during the dynamic process of wound healing, promoting effective tissue repair.[26] Tissue fluidity enables epithelial cells to transition from a solid-like to a fluid-like biophysical state, supporting cellular activation crucial for processes like re-epithelialization and tissue regeneration, essential for skin integrity restoration.[27] For instance, Sarate et al elucidated the role of the EGFR/AP1 pathway in regulating tissue fluidity and aiding skin repair.[16] Their work illustrated that EGFR ligand secretion, particularly EREG, activates the EGFR/AP1 pathway, pivotal in processes such as cell proliferation, re-epithelialization, and tissue regeneration. In our study, we focused on genes associated with the EGFR-AP-1 axis and tissue fluidity, targeting EGFR, EREG, MAP2K1, MAP2K2, JUN, JUNB, FOS, and FOSB. Our investigation revealed significant downregulation of FOS and JUNB in the DFUs healing group but upregulation in the non-healing group. Additionally, Wang et al highlighted the impact of intercellular adhesion levels on tissue fluidization, prompting our analysis of MYH9 and CDH1, genes linked to cell adhesion. Interestingly, MYH9 exhibited high expression in the DFUs healing group.[28] Enrichment analysis further unveiled that elevated FOS expression in DFUs patients influences cell differentiation and the p53-mediated p21 signaling pathway functions.

Thirdly, CDKN1A is critical in different skin diseases and cellular processes. For instance, CDKN1A has been linked to melanoma[29] and cellular senescence across tissues, including skin cell senescence.[30] CDKN1A is crucial for inducing cell cycle arrest and maintaining the senescence phenotype.[31] Cellular senescence, in turn, is associated with chronic age-related conditions, including DFUs.[32] DFUs exhibit higher expression of genes and pathways related to senescence compared to non-DFUs cases.[33,34] Additionally, Yu et al demonstrated that elevated CDKN1A expression is linked to wound chronicity, with diabetic wounds showing increased levels of senescence.[35] In this study, we conducted a reclustering analysis of BasalKera cells from both DFUs healing and non-healing groups and observed that FOS exhibited higher expression in clusters predominantly associated with the non-healing group, whereas MKI67 displayed elevated expression in clusters more prevalent in the healing group. Additionally, clusters with a higher proportion of cells from the non-healing group showed significant enrichment of genes involved in cell differentiation and the p53 signaling pathway. We further constructed a network diagram of core genes related to keratinocyte differentiation and p53 signal transduction, identifying that both CDKN1A and TP63 play roles in these pathways, with CDKN1A serving as a central gene in the p21 pathway.

MR has been widely applied to uncover the molecular mechanisms underlying complex diseases, including diabetes,[36] cardiovascular diseases,[13] and osteoarthritis.[37] In their study, Yin et al utilized MR to identify causal relationships between specific risk factors, such as elevated HbA1c levels, reduced HDL cholesterol, and an increased risk of DFUs.[38] Furthermore, a recent study employing MR investigated the causal effects of type 2 diabetes on 67

neurological conditions and identified significant associations with several peripheral neuropathies, including carpal tunnel syndrome, cervical root disorders, and Bell's palsy. These findings support a causal role of T2D in peripheral nerve dysfunction and highlight the utility of MR in disentangling complex metabolic-neurological relationships.[39] By integrating genetic and phenotypic data, MR provides a robust framework for pinpointing key genes and metabolic pathways that drive disease processes.[40] Here, we conducted an MR analysis to explore the causal relationship between 1400 metabolites and DFUs and performed SMR analysis to assess the relationship between CDKN1A and DFUs, as well as between CDKN1A and the 43 metabolites identified as having causal relationships with DFUs. SMR results for the eQTL of CDKN1A and the 43 metabolites revealed a causal relationship between CDKN1A and the ratio of α-ketobutyrate to pyruvate. Thus, CDKN1A impacts DFUs wound healing through its role in energy metabolism.

Pseudotime analysis was employed to investigate the differentiation trajectories of BasalKera and DiffKera cells in DFUs healing and non-healing groups. Our analysis revealed that BasalKera cells in the non-healing group exhibited higher differentiation states, but fewer fully differentiated DiffKera cells compared to the healing group. This indicated abnormal differentiation and incomplete functionality of keratinocytes in non-healing DFUs, potentially linked to impaired energy metabolism. Additionally, CDKN1A expression was found to increase along differentiation trajectories, with higher levels in the non-healing group. Transcription factor analysis revealed that FOS and JUNB had stronger regulatory roles in the non-healing group, influencing CDKN1A expression. Validation using the cistrome database confirmed that both FOS and JUNB regulate CDKN1A, with FOS showing a stronger regulatory effect.

Although these are active results, some limitations here we also admitted. While scRNA-seq and MR provided crucial insights into the molecular mechanisms underlying DFUs healing, these techniques are inherently observational. Experimental validation through in vitro and in vivo studies is necessary to confirm the causal roles of the identified genes, such as CDKN1A, and pathways, including the EGFR-AP-1 axis, in tissue fluidity and wound healing. Another limitation is that while the study focused on the key role of CDKN1A in energy metabolism and its regulation by transcription factors FOS and JUNB, other potentially significant regulators and pathways may have been overlooked. Investigating other transcription factors or epigenetic modifications that influence CDKN1A expression could yield further insights.

Future studies should aim to validate the functional role of CDKN1A and its upstream regulators, particularly FOS, using in vitro experiments with keratinocytes and in vivo diabetic wound models. Combining additional biological data types such as protein expression, gene regulation patterns, and location-based gene activity in tissues may help reveal when and where key healing processes occur in diabetic wounds. Investigating the potential of CDKN1A-targeted therapeutics or transcription factor modulators may also open new avenues for personalized treatment of DFU. Furthermore, translating these findings into clinical settings through prospective cohort studies or drug development pipelines could significantly advance wound care strategies.

Conclusion

In this study, we combined scRNA-seq and MR to explore the molecular mechanisms underlying DFU healing. Our findings emphasized the critical roles of tissue fluidity, CDKN1A, and associated transcriptional and metabolic pathways in DFU healing. Specifically, we identified how CDKN1A influences tissue fluidity and energy metabolism and uncovered its regulation by key transcription factors like FOS and JUNB. Additionally, we established a causal link between CDKN1A and the α-ketobutyrate/pyruvate ratio through MR analysis. In summary, our results demonstrated that CDKN1A significantly impacts DFU wound healing through its role in energy metabolism, offering potential targets for therapeutic intervention.

Abbreviations

DFUs, Diabetic foot ulcers; ROS, excessive reactive oxygen species; scRNA-seq, single-cell RNA sequencing; ST, spatial transcriptomics; GEO, Gene Expression Omnibus; CDKN1A, cyclin-dependent kinase inhibitor 1A; HG, high glucose; T2DM, Type 2 Diabetes Mellitus; MR, Mendelian randomization; eQTL, expression quantitative trait loci; UKB, UK Biobank; QC, quality control; PCA, principal component analysis; BasalKera, basal keratinocytes; DEGs, differentially expressed genes; GO, Gene Ontology; BP, biological processes; GSEA, Gene Set Enrichment Analysis;

PCs, principal components; GO.BP, Gene Ontology biological processes; IVW, Inverse Variance Weighted; DiffKera, differentiating keratinocytes; SMC, smooth muscle cells; VasEndo, vascular endothelial cells; Sweat/Seba, sweat/sebaceous glands; LymphEndo, lymphatic endothelial cells; Melano/Schwann, melanocytes/Schwann cells; UMAP, Uniform Manifold Approximation and Projection; MYH9, non-muscle myosin II; CDH1, classical cadherin; SMR, Summary-data-based Mendelian Randomization.

Data Sharing Statement

The scRNA-seq dataset (GSE165816) for DFUs was downloaded from the GEO database (https://www.ncbi.nlm.nih.gov/gds). For MR analysis, the outcome phenotype was DFUs, with relevant data obtained from the UK Biobank (UKB) database. The exposure of interest was CDKN1A, with its eQTL data sourced from the IEU OpenGWAS database (https://gwas.mrcieu.ac.uk/). A dataset containing 1400 plasma metabolites was sourced from the GWAS Catalog (ID: GCST90199621-90201020).

Ethics Approval and Consent to Participate

This study utilized publicly available data from open-access databases, and no new human data were collected or generated. According to national legislation in China, specifically Item 1 and Item 2 of Article 32 of the Measures for Ethical Review of Life Science and Medical Research Involving Human Subjects (effective February 18, 2023), research involving publicly available data does not require additional ethical approval or informed consent. Therefore, this study is exempt from review by an Institutional Review Board (IRB).

Author Contributions

All authors made a significant contribution to the work reported, whether that is in the conception, study design, execution, acquisition of data, analysis and interpretation, or in all these areas; took part in drafting, revising or critically reviewing the article; gave final approval of the version to be published; have agreed on the journal to which the article has been submitted; and agree to be accountable for all aspects of the work.

Funding

This work was financially supported by Natural Science Foundation of Hubei Province (2022CFB298), Innovation Fund for Industry-University-Research of Chinese Universities (2021ITA03006), Wuhan University Education and Development Foundation (NO.2002330) Public Hygiene and Health Commission of Shenzhen Municipality of Integration of Medical and Preventive Services with Traditional Chinese Medicine Group Project ([2019]No.25).

Disclosure

The authors report no conflicts of interest in this work.

References

1. Mariadoss AVA, Sivakumar AS, Lee CH, Kim SJ. Diabetes mellitus and diabetic foot ulcer: etiology, biochemical and molecular based treatment strategies via gene and nanotherapy. *Biomed Pharmacother Biomedecine Pharmacother*. 2022;151:113134. doi:10.1016/j.biopha.2022.113134
2. Armstrong DG, Tan TW, Boulton AJM, Bus SA. Diabetic foot ulcers: a review. *JAMA*. 2023;330(1):62–75. doi:10.1001/jama.2023.10578
3. Wang Y, Shao T, Wang J, et al. An update on potential biomarkers for diagnosing diabetic foot ulcer at early stage. *Biomed Pharmacother Biomedecine Pharmacother*. 2021;133:110991. doi:10.1016/j.biopha.2020.110991
4. Aghayants S, Zhu J, Yu J, et al. The emerging modulators of non-coding RNAs in diabetic wound healing. *Front Endocrinol*. 2024;15:1465975. doi:10.3389/fendo.2024.1465975
5. Zhu Z, Zhou S, Li S, Gong S, Zhang Q. Neutrophil extracellular traps in wound healing. *Trends Pharmacol Sci*. 2024;45(11):1033–1045. doi:10.1016/j.tips.2024.09.007
6. Shi T, Lu H, Zhu J, et al. Naturally derived dual dynamic crosslinked multifunctional hydrogel for diabetic wound healing. *Compos Part B Eng*. 2023;257:110687. doi:10.1016/j.compositesb.2023.110687
7. Huang B, An H, Chu J, et al. Glucose-responsive and analgesic gel for diabetic subcutaneous abscess treatment by simultaneously boosting photodynamic therapy and relieving hypoxia. *Adv Sci*. 2025. doi:10.1002/advs.202502830
8. Jovic D, Liang X, Zeng H, Lin L, Xu F, Luo Y. Single-cell RNA sequencing technologies and applications: a brief overview. *Clin Transl Med*. 2022;12(3):e694. doi:10.1002/ctm2.694
9. Theocharidis G, Thomas BE, Sarkar D, et al. Single cell transcriptomic landscape of diabetic foot ulcers. *Nat Commun*. 2022;13(1):181. doi:10.1038/s41467-021-27801-8

10. Su J, Wei Q, Ma K, et al. P-MSC-derived extracellular vesicles facilitate diabetic wound healing via miR-145-5p/ CDKN1A-mediated functional improvements of high glucose-induced senescent fibroblasts. *Burns Trauma*. 2023;11:tkad010.
11. Engeland K. Cell cycle regulation: p53-p21-RB signaling. *Cell Death Differ*. 2022;29(5):946–960. doi:10.1038/s41418-022-00988-z
12. Muhammad SA, Qousain Naqvi ST, Nguyen T, et al. Cisplatin's potential for type 2 diabetes repositioning by inhibiting CDKN1A, FAS, and SESN1. *Comput Biol Med*. 2021;135:104640. doi:10.1016/j.compbiomed.2021.104640
13. Larsson SC, Butterworth AS, Burgess S. Mendelian randomization for cardiovascular diseases: principles and applications. *Eur Heart J*. 2023;44 (47):4913–4924. doi:10.1093/eurheartj/ehad736
14. Emdin CA, Khera AV, Kathiresan S. Mendelian Randomization. *JAMA*. 2017;318(19):1925–1926. doi:10.1001/jama.2017.17219
15. Burgess S, Woolf B, Mason AM, Ala-Korpela M, Gill D. Addressing the credibility crisis in Mendelian randomization. *BMC Med*. 2024;22(1):374. doi:10.1186/s12916-024-03607-5
16. Sarate RM, Hochstetter J, Valet M, et al. Dynamic regulation of tissue fluidity controls skin repair during wound healing. *Cell*. 2024;187(19):5298–5315.e19. doi:10.1016/j.cell.2024.07.031
17. Visker JR, Cluntun AA, Velasco-Silva JN, et al. Enhancing mitochondrial pyruvate metabolism ameliorates ischemic reperfusion injury in the heart. *JCI Insight*. 2024;9(17):e180906. doi:10.1172/jci.insight.180906
18. Cluntun AA, Badolia R, Lettlova S, et al. The pyruvate-lactate axis modulates cardiac hypertrophy and heart failure. *Cell Metab*. 2021;33(3):629–648.e10. doi:10.1016/j.cmet.2020.12.003
19. Xu Y, Ouyang C, Lyu D, et al. Diabetic nephropathy execrates epithelial-to-mesenchymal transition (EMT) via miR-2467-3p/Twist1 pathway. *Biomed Pharmacother Biomedecine Pharmacother*. 2020;125:109920. doi:10.1016/j.biopha.2020.109920
20. Senneville É, Albalawi Z, van Asten SA, et al. IWGDF/IDSA guidelines on the diagnosis and treatment of diabetes-related foot infections (IWGDF/IDSA 2023). *Diabetes Metab Res Rev*. 2024;40(3):e3687. doi:10.1002/dmrr.3687
21. Zhu ML, Fan JX, Guo YQ, et al. Protective effect of alizarin on vascular endothelial dysfunction via inhibiting the type 2 diabetes-induced synthesis of THBS1 and activating the AMPK signaling pathway. *Phytomedicine Int J Phytother Phytopharm*. 2024;128:155557.
22. Wu B, Pan W, Luo S, et al. Turmeric-derived nanoparticles functionalized aerogel regulates multicellular networks to promote diabetic wound healing. *Adv Sci Weinh Baden-Wurtt Ger*. 2024;11(18):e2307630.
23. Shi H, Song H, Wu Q, Liu L, Song Z, Gu Y. Relationship between immune cell traits, circulating inflammatory cytokines, and the risk of incisional hernia after gastric surgery. *Hernia J Hernias Abdom Wall Surg*. 2024;29(1):27. doi:10.1007/s10029-024-03213-7
24. Loibl S, Poortmans P, Morrow M, Denkert C, Curigliano G. Breast cancer. *Lancet Lond Engl*. 2021;397(10286):1750–1769. doi:10.1016/S0140-6736(20)32381-3
25. Chen RF, Lin YN, Liu KF, et al. Compare the effectiveness of extracorporeal shockwave and hyperbaric oxygen therapy on enhancing wound healing in a streptozotocin-induced diabetic rodent model. *Kaohsiung J Med Sci*. 2023;39(11):1135–1144. doi:10.1002/kjm2.12746
26. Tetley RJ, Staddon MF, Heller D, Hoppe A, Banerjee S, Mao Y. Tissue fluidity promotes epithelial wound healing. *Nat Phys*. 2019;15 (11):1195–1203. doi:10.1038/s41567-019-0618-1
27. C Z, C Z, Rinkevich Y. Tissue fluidity: biophysical shape-shifting for regeneration. *Signal Transduct Target Ther*. 2024;9(1):329. doi:10.1038/s41392-024-02068-9
28. Wang X, Cupo CM, Ostvar S, Countryman AD, Kasza KE. E-cadherin tunes tissue mechanical behavior before and during morphogenetic tissue flows. *Curr Biol CB*. 2024;34(15):3367–3379.e5. doi:10.1016/j.cub.2024.06.038
29. Chen L, Fang C, Yuan X, et al. Has-miR-300-GADD45B promotes melanoma growth via cell cycle. *Aging*. 2023;15(23):13920–13943. doi:10.18632/aging.205276
30. Yu GT, Ganier C, Allison DB, et al. Mapping epidermal and dermal cellular senescence in human skin aging. *Aging Cell*. 2024;24(1):e14358. doi:10.1111/acel.14358
31. Xu P, Wang M, Song WM, et al. The landscape of human tissue and cell type specific expression and co-regulation of senescence genes. *Mol Neurodegener*. 2022;17(1):5. doi:10.1186/s13024-021-00507-7
32. Samarawickrama PN, Zhang G, Zhu E, et al. Clearance of senescent cells enhances skin wound healing in type 2 diabetic mice. *Theranostics*. 2024;14(14):5429–5442. doi:10.7150/thno.100991
33. Wilkinson HN, Clowes C, Banyard KL, Matteuci P, Mace KA, Hardman MJ. Elevated local senescence in diabetic wound healing is linked to pathological repair via CXCR2. *J Invest Dermatol*. 2019;139(5):1171–1181.e6. doi:10.1016/j.jid.2019.01.005
34. Wilkinson HN, Hardman MJ. Senescence in wound repair: emerging strategies to target chronic healing wounds. *Front Cell Dev Biol*. 2020;8:773. doi:10.3389/fcell.2020.00773
35. Yu GT, Monie DD, Khosla S, Tchkonia T, Kirkland JL, Wyles SP. Mapping cellular senescence networks in human diabetic foot ulcers. *GeroScience*. 2024;46(1):1071–1082. doi:10.1007/s11357-023-00854-x
36. Goto A, Yamaji T, Sawada N, et al. Diabetes and cancer risk: a mendelian randomization study. *Int, J, Cancer*. 2020;146(3):712–719. doi:10.1002/ijc.32310
37. Ho J, Mak CCH, Sharma V, To K, Khan W. Mendelian randomization studies of lifestyle-related risk factors for osteoarthritis: a PRISMA review and meta-analysis. *Int J Mol Sci*. 2022;23(19):11906. doi:10.3390/ijms231911906
38. Yin K, Qiao T, Zhang Y, et al. Unraveling shared risk factors for diabetic foot ulcer: a comprehensive Mendelian randomization analysis. *BMJ Open Diabetes Res Care*. 2023;11(6):e003523. doi:10.1136/bmjdrc-2023-003523
39. Wei Y, Xu S, Wu Z, Zhang M, Bao M, He B. Exploring the causal relationships between type 2 diabetes and neurological disorders using a mendelian randomization strategy. *Medicine*. 2024;103(46):e40412. doi:10.1097/MD.0000000000040412
40. Davies NM, Holmes MV, Davey Smith G. Reading Mendelian randomisation studies: a guide, glossary, and checklist for clinicians. *BMJ*. 2018;362:k601. doi:10.1136/bmj.k601